I. Structure-based design, synthesis and structure-activity relationship of D-Phe-Pro-D-Arg-P1"-CONH2 peptides inhibitors for thrombin. II. DNA translesion synthesis of mitomycin C...

THESIS · JANUARY 2006

1 AUTHOR:

Cristina Clement
Albert Einstein College of Medicine
59 PUBLICATIONS **934** CITATIONS

SEE PROFILE

DNA Adduct of the Mitomycin C Metabolite 2,7-Diaminomitosene Is a Nontoxic and Nonmutagenic DNA Lesion in Vitro and in Vivo

Christopher D. Utzat,[†,‡] Cristina C. Clement,[‡,§] Leilani A. Ramos,[†] Arunangshu Das,[§,||] Maria Tomasz,[*,§] and Ashis K. Basu[*,†]

Department of Chemistry, University of Connecticut, Storrs, Connecticut 06269, and Department of Chemistry, Hunter College, City University of New York, New York, New York 10021

Received July 13, 2004

Mitomycin C (MC) is a cytotoxic and mutagenic antitumor agent that alkylates and cross-links DNA. These effects are dependent on reductive bioactivation of MC. 2,7-Diaminomitosene (2,7-DAM) is the major metabolite of MC in tumor cells, generated by the reduction of MC. 2,7-DAM alkylates DNA in the cell in situ, forming an adduct at the N7 position of 2′-deoxyguanosine (2,7-DAM-dG-N7). To determine the biological effects of this adduct, we have synthesized an oligonucleotide containing a single 2,7-DAM-dG-N7 adduct and inserted it into an M13 bacteriophage genome. Replication of this construct in repair-competent *Escherichia coli* showed that the adduct was only weakly toxic and generated ∼50% progeny as compared to control. No mutant was isolated after analysis of more than 4000 progeny phages from SOS-induced or uninduced host cells; therefore, we estimate that the mutation frequency of 2,7-DAM-dG-N7 was less than 2×10^{-4} in *E. coli*. Subsequently, to determine if this adduct might be mutagenic in mammalian cells, it was incorporated into a single-stranded shuttle phagemid vector, pMS2, and replicated in simian kidney (COS-7) cells. Analysis of the progeny showed that mutational frequency of a site specific 2,7-DAM-dG-N7 was not higher than the spontaneous mutation frequency in simian kidney cells. In parallel experiments in cell free systems, template oligonucleotides containing a single 2,7-DAM-dG-N7 adduct directed selective incorporation of cytosine in the 5′-^{32}P-labeled primer strands opposite the adducted guanine, catalyzed by Klenow (exo-) DNA polymerase. The adducted templates also supported full extension of primer strands by Klenow (exo$^-$) and T7 (exo$^-$) DNA polymerases and partial extension by DNA polymerase η. The innocuous behavior of the 2,7-DAM-dG-N7 monoadduct in vivo and in vitro is in sharp contrast to that of the toxic MC-dG-N^2 monoadduct reported earlier.

Introduction

Mitomycin C (MC;[1] **1**, Scheme 1) is an antitumor antibiotic used clinically as a chemotherapeutic agent against several types of cancer (*1*). 2,7-Diaminomitosene (2,7-DAM; **2**) is a major metabolite found in cells and tissues treated with MC (*2*, *3*). The antitumor activity of MC is believed to be based on its ability to alkylate DNA to form several monofunctional adducts and cross-links in DNA (*4*). MC requires reductive activation for the DNA alkylation process (*5*). However, the activated hydroquinone species **3** is partitioned between the pathway of DNA alkylation and a predominant metabolic pathway,

Scheme 1. MC and 2,7-DAM

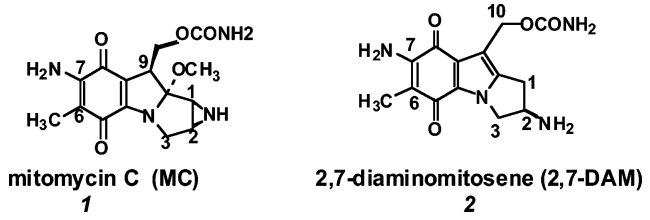

Scheme 2. (a) Reductive Metabolism of MC and (b) Reductive Alkylation of DNA by 2,7-DAM

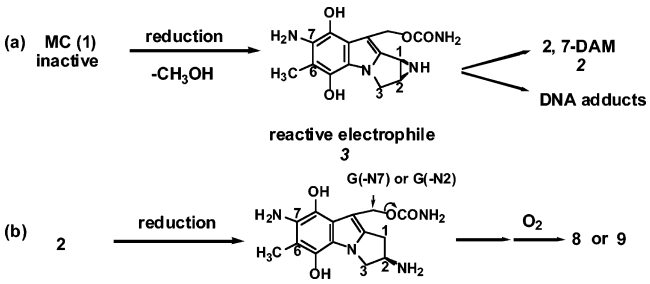

which produces a new quinone, 2,7-DAM (Scheme 2a; *2*, *3*, *6*). In MC-treated tumor cells, six major covalent DNA adducts are formed and the same six adducts can be isolated in reconstituted cell-free systems using flavore-

* To whom correspondence should be addressed. (M.T.) Tel: 212-772-5387. Fax: 212-772-5332. E-mail: mtomasz@hunter.cuny.edu. (A.K.B.) Tel: 860-486-3965. Fax: 860-486-2981. E-mail: ashis.basu@uconn.edu.

† University of Connecticut.

‡ These authors contributed equally to this work.

§ City University of New York.

|| Current address: Department of Biochemistry and Molecular Biology, Penn State College of Medicine, 500 University Drive, Hershey, PA 17033.

[1] Abbreviations: *A*, absorbance; 2,7-DAM, 2,7-diaminomitosene; DMS, dimethyl sulfate; E, enzyme; ESI-MS (−), electrospray ionization mass spectroscopy (negative mode); MC, mitomycin C; nt, nucleotide; PAGE, polyacrylamide gel electrophoresis; PNK, T4 polynucleotide kinase; S, substrate; TEAA, triethylammonium acetate; TLS, translesion synthesis; UDG, uracil DNA glycosylase.

10.1021/tx049813h CCC: $30.25
Published on Web 01/15/2005

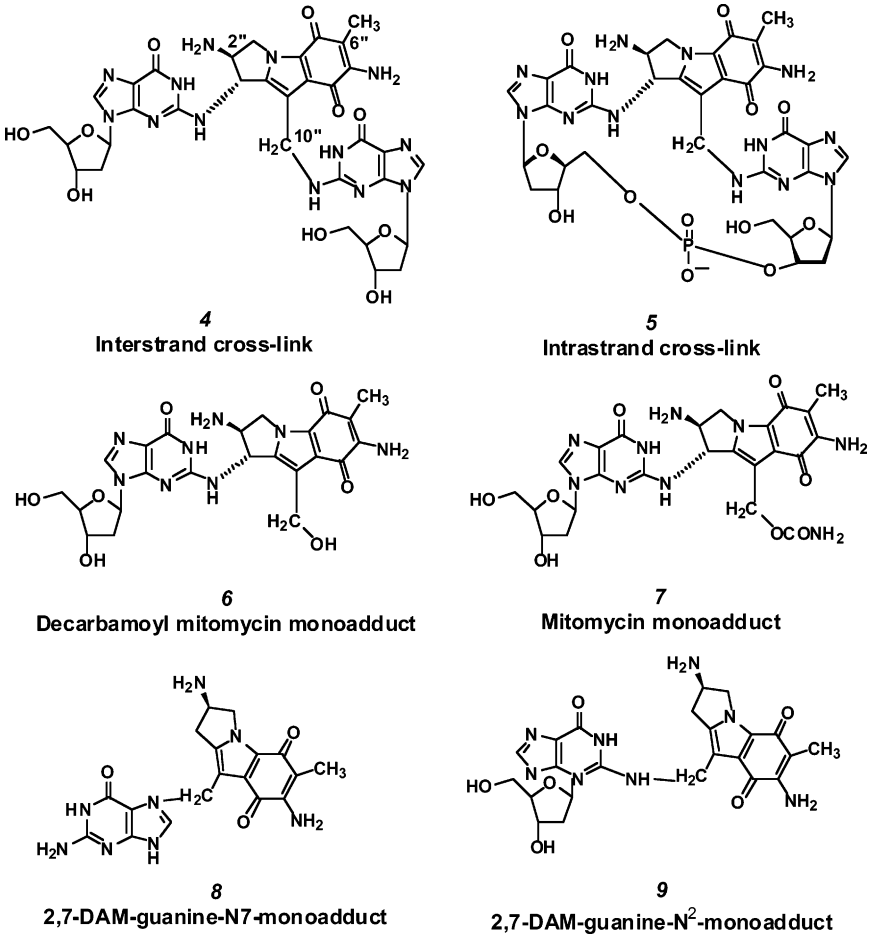

Figure 1. Six major DNA adducts of reductively activated MC.

ductases or chemical reducing agents for activation of the drug. The structures of the DNA adducts are shown in Figure 1. Four of the six adducts (**4**−**7**) are generated directly from the active form of MC by alkylation of the 2-amino group of guanine in the minor groove of DNA to give both monofunctional (**6**, **7**) and bifunctional (**4**, **5**) DNA adducts (*7*). Adducts **8** and **9** are products of 2,7-DAM. This was shown by direct treatment of the cells or DNA in vitro with purified 2,7-DAM itself, which resulted in the selective formation of adducts **8** and **9**, at high efficiency. 2,7-DAM lacks the aziridine ring and alkylates DNA monofunctionally at the guanine-N7 and -N^2 positions (Scheme 2b). The alkylation, like with MC, requires reductive activation; the relative proportions of the two adducts vary, depending on the conditions of their formation (*7*, *8*).

Comparison of the cytotoxicities of MC and 2,7-DAM to tumor cells revealed that 2,7-DAM is only mildly cytotoxic in contrast to the intensely cytotoxic parent compound, MC (*9*, *10*). Paralleling the relative cytotoxicities, 2,7-DAM was found to be nonmutagenic in a *Salmonella* tester system.[2]

Because only the parent drug MC has DNA cross-linking activity, one may expect MC to be more cytotoxic and mutagenic than its metabolite, the purely monofunctional DNA alkylator 2,7-DAM. Nevertheless, the almost total lack of biological activity of the latter was surprising, especially in light of the fact that other monofunctional DNA alkylating natural products, e.g., aflatoxin B_1, anthramycin, CC-1065, etc., are strongly mutagenic and/or cytotoxic (*11*, *12*).

Relationships between DNA adduct structure and activity are generally not well-understood. The lack of biological activity of 2,7-DAM, combined with our detailed knowledge of the structure of its major DNA adduct **8**, offered a well-defined system to study such a relationship of an abundantly formed bulky DNA adduct, and this is the major subject of this study. Direct comparison with the major mitomycin monoadduct **7**, which has well-defined contrasting structural properties, was included in the investigation. A comparison of the biological effects of the adducts of MC and 2,7-DAM is important for a better understanding of the in vivo effects of MC itself. Specifically, we examined the effects of the major monoadducts of MC and 2,7-DAM on phage viability and mutagenesis and on the fidelity and efficiency of DNA replication in biochemical model systems.

Experimental Procedures

MC was obtained from Dr. Dinesh M. Vyas, Bristol Myers Squibb Co. (Wallingford, CT). 2,7-DAM was obtained by reduction of MC with H_2/PtO_2 as previously described (*3*). [γ-^{32}P]ATP was from DuPont New England Nuclear (Boston, MA) or from Perkin-Elmer Life Sciences (3000 Ci/mmol, 10 mCi/mL). T4 DNA ligase (400 units/μL) and T4 polynucleotide kinase (PNK) (10 000 units/mL) were obtained from New England Biolabs (Beverly, MA). Phosphodiesterase I (snake venom diesterase, *Crotalus adamanteus* venom, EC 3.1.4.1) and alkaline phos-

[2] This test was conducted by the commercial testing service MA Bioservices, Inc. (Rockville, MD).

phatase (*Escherichia coli*, EC 3.1.3.1) were obtained from Worthington Biochemical Corp. (Freehold, NJ). *E. coli* Klenow (exo) DNA polymerase (5000 units/mL) was purchased from USB (Cleveland, OH). Exonuclease-free T7 (exo-) DNA polymerase (13 units/μL) was either purchased from USB or was a gift from Dr. Smita Patel (UMDNJ, Piscataway, NJ) and was active site titrated using the quench-flow instrument in the same lab (>75% active enzyme). DNA polymerase η, the full length clone of the human enzyme containing a C-terminal 6X histidine tag, was a generous gift from Dr. Scott McCulloch and Dr. Thomas A. Kunkel (Laboratories of Molecular Genetics and Structural Biology, NIEHS, NIH, Research Triangle Park, NC). *E. coli* strains DL7 and GW5100 and simian kidney COS-7 cells were available in the Basu laboratory. Synthetic oligonucleotides were purchased from the Midland Certified Reagent Company, Inc. (Midland, TX) or were synthesized in the Core Facilities at Hunter College and further purified and desalted through a Sephadex G-25 column. Their purity was confirmed through reversed phase HPLC and negative electrospray ionization mass spectroscopy ESI-MS (−).

Methods. UV spectra and absorbance readings were recorded in a Cary 3 UV−visible spectrophotometer. Alternatively, the absorbance readings were obtained in a Gilford 250 spectrophotometer. All DNA concentrations were determined by using the calculated molar extinction coefficient [E_{260} (strand)] for each oligonucleotide strand, and the absorbance readings were obtained at 260 nm using the formula: $c = A_{260}/[E_{260}\ (\text{strand}) \times L]$ (where the molar extinction coefficient E is expressed in $M^{-1}\ cm^{-1}$ and the path length of the cuvette is $L = 1.0$ cm). Each E_{260} (strand) was calculated using the formula: E_{260} (strand) = number of purines × 14 000 + number of pyrimidines × 7000, where 14 000 and 7000 are the averaged molar extinction coefficients for purines and for pyrimidines, respectively (*15*). In the case of the 2,7-DAM alkylated oligonucleotide, a correction for E_{260} (strand) was done by adding 5189 (E_{260} of 2,7-DAM) (*13*). LC-MS was performed with a Hewlett-Packard series 1100 diode array HPLC system connected to a Hewlett-Packard series 1100 MSD mass spectrometer. HPLC was performed in a Beckman System Gold 125 instrument, equipped with a Beckman System Gold 168 diode array detector. The HPLC columns used for analytical purposes were C18, 100 Å (Microsorb MV Rainin, 5 mm × 250 mm) and C4, 300 Å (Microsorb MV Rainin, 5 mm × 250 mm) while the columns for semipreparative and preparative use were C18, 100 Å, Dynamax (5 μm, 1 cm × 25 cm) and C4, 300 Å, Dynamax (5 μm, 2.14 cm × 25 cm), respectively. Polyacrylamide gel electrophoresis (PAGE) (18%) with 8 M urea was run in a Sequi-Gen GT (Biorad Inc., CA) apparatus, at 2800 constant voltage for 3.5 h. The gel was exposed to phosporimaging on a Phosphorimager 445 SI (Molecular Dynamics, now Amersham Biosciences), and the quantitative data were produced using the software ImageQuant 5.2.

Synthesis of the Site Specifically Substituted Short Oligonucleotides 10−13 (Scheme 3). Synthetic oligonucleotides were incubated with MC or 2,7-DAM under reductive conditions using $Na_2S_2O_4$ or catalytic hydrogenation in aqueous buffer, as described earlier. Specifically, 9-mer **10** and the 10-mer **11** were synthesized and characterized as reported (*13*, *15*, respectively). The new oligonucleotides **12** and **13** were prepared and characterized using a modified procedure described originally for **11**. Briefly, the reaction of alkylation was performed in 0.1 M potassium phosphate buffer, pH 5.5, in the presence of PtO_2 as catalyst, under anaerobic conditions. A total of 168 OD_{260} units of oligonucleotide mixture containing either the unsubstituted oligonucleotide precursor of **12** annealed with 3′-GACCATTAA-5′ or the unsubstituted oligonucleotide precursor of **13** annealed with 5′-GGATACCACT-3′ were mixed with 4.2 μmol of 2,7-DAM and 0.841 mg of PtO_2 in 5 mL of 0.1 M potassium phosphate buffer, pH 5.5, and the mixture was annealed by heating it at 95 °C for 3 min, then slowly cooled to 25 °C, followed by keeping it on ice for 30 min. After the mixture was annealed, solid ferrous ammonium sulfate (0.084 mg) was added to the mixture and then purged with argon for 15 min. The hydrogenation was performed by purging with H_2 for 17 min at room temperature. After it was purged with argon for 1 h at room temperature, the reaction mixture was exposed to air and was applied on Sephadex G-25 fine column. The first UV-absorbing peak containing the unmodified and modified oligonucleotides was collected, and further purification of alkylated oligos was performed using a semipreparative C18, column, 300 Å, and the following elution system. Eluant A: 30 mM phosphate, pH 5.4; eluant B: 30% CH_3CN in 70% 30 mM phosphate, pH 5.4. The gradient used was 10−25% B in 10 min, 25−33% B in 60 min, and 33−100% B in 20 min, with a 3 mL/min flow rate. The absorbance was recorded at both 260 and 314 nm, and the adducted oligos were identified from their absorption at both wavelengths and collected as described (*15*).

Scheme 3. Alkylated Oligonucleotides (10−13) and Oligonucleotide Templates (14−16) Constructed by Ligation[a]

5′-ACACG(MC)TCAT-3′ **10** (9-mer)

5′-GTGG(2,7-DAM)TACCAC-3′ **11** (10-mer)

5′-CTGG(2,7-DAM)TAATTTAC-3′ **12** (12-mer)

5′-CTAGTGG(2,7-DAM)TATCC-3′ **13** (12-mer)

5′-ACACG(MC)TCATTAGAGATTGGTAGGG-3′ **14** (24-mer)

5′-CTGG(2,7-DAM)TAATTTACTAGAGATTGGTAGGG-3′ **15** (27-mer)

5′-CTAGTGG(2,7-DAM)TATCCTAGAGATTGGTA-3′ **16** (24-mer)

[a] The drug-modified nt unit G(MC) corresponds to MC adduct **7**, and the drug-modified unit G(2,7-DAM) corresponds to 2,7-DAM adduct **8** (Figure 1) throughout.

Characterization of Adducted Oligonucleotides 10−13. In general, analytical HPLC was used to establish homogeneity, using reverse phase columns [Rainin C4 column, 300 Å (Rainin Microsorb MV, 5 mm × 250 mm)]. ESI-MS (−) confirmed the molecular weight of the adducted oligonucleotides. Digestion by snake venom phosphodiesterase and alkaline phosphatase, followed by reverse phase HPLC of the digest, confirmed the structure of the nucleoside adduct **7** in oligonucleotide **10**, adduct **8** in oligonucleotides **11**−**13**, and the nucleoside and drug-nucleoside adduct composition of **10**−**13** as described before (*13*, *15*).

Position of the 2,7-DAM Adduct 8 in Oligonucleotides 11−13. There are two guanines in **11** and **12** and three guanines in **13**. The positions of the adducts were determined as follows. For compound **11**, the oligonucleotide was 5′-labeled with [^{32}P], heated in hot piperidine, and analyzed by PAGE along a Maxam−Gilbert G-lane of labeled unmodified control oligonucleotide. The results showed that **11** was substituted exclusively at G(4) as described in detail earlier (*15*). Positions in **12** and **13** were determined analogously.

Construction of Alkylated Templates 14−16. The short adducted oligonucleotides **10**−**13** (6 nmol each) were ligated to 5′-phosphorylated oligonucleotides (6 nmol each) by T4 DNA ligase (400 units/6 nmol duplex DNA) in the presence of a complementary oligomer (6 nmol), which held the ligating oligomers together, using a modified procedure described originally for other mitomycin-adducted constructs (*13*). The ligation reaction for the MC-adducted construct **14** was performed for 6 h at room temperature while the ligation reactions for the 2,7-DAM-adducted constructs **15** and **16** were performed for 16 h at room temperature. Specific oligonucleotide components used for the construction of each template were the following: 24-mer template (**14**): **10**, 5′-pTAGAGATTGGTAGGG, 5′-ACCAATCTCTAATGACGTGT. 27-mer template (**15**): **12**, 5′-pTAGAGATTGGTAGGG, 5′-AATCTCAGTAAATTAC. 24-mer template (**16**): **13**, 5′-pTAGAGATTGGTA, 5′-CCAATCTCTAGGATACCACT.

Scheme 4. Primer−Template Complexes 17−22 Used in Primer Extension on Adducted Templates[a]

3'-ATCTCTAACCATCCC-5'-^{32}P (15-mer)
5'-ACACG(MC)TCATTAGAGATTGGTAGGG-3' (24-mer)
17

3'-AATGATCTCTAACCAT-5'-^{32}P (16-mer)
5'-CTGG(2,7-DAM)TAATTTACTAGAGATTGGTAGGG-3' (27-mer)
18

3'-AGGATCTCTAACCAT-5'-^{32}P (15-mer)
5'-CTAGTGG(2,7-DAM)TATCCTAGAGATTGGTA-3' (24-mer)
19

3'-AGTAATCTCTAACCATCCC-5'-^{32}P (19-mer)
5'-ACACG(MC)TCATTAGAGATTGGTAGGG-3' (24-mer)
20

3'-ATTAAATGATCTCTAACCATCCC-5'-^{32}P (23-mer)
5'-CTGG(2,7-DAM)TAATTTACTAGAGATTGGTAGGG-3' (27-mer)
21

3'-ATAGGATCTCTAACCAT-5'-^{32}P (17-mer)
5'-CTAGTGG(2,7-DAM)TATCCTAGAGATTGGTA-3' (24-mer)
22

[a] The drug-modified nt unit G(MC) corresponds to MC adduct **7**, and the drug-modified unit G(2,7-DAM) corresponds to 2,7-DAM adduct **8** (Figure 1) throughout.

The constructed alkylated templates **14**−**16** were purified from the other oligonucleotides in the ligation mix using a 16% polyacrylamide−8 M urea gel. The templates were detected by UV shadowing and excised from the gel, and the gel pieces were soaked overnight at room temperature in 100 mM Tris, 0.5 M NaCl, and 5 mM EDTA, pH 8.0. The templates were desalted by passing through a C18-Sep-Pak cartridge (Waters). The elution buffer consisted of 0.1 M triethylammonium acetate (TEAA), pH 7.0:100% CH_3OH (1:1). The alkylated templates were analyzed for the presence of the MC or 2,7-DAM adduct by digestion with snake venom phosphodiesterase and alkaline phosphatase followed by analysis of the digests by HPLC, as described for characterization of the short oligonucleotides **10**−**13** above.

The purity of the alkylated templates was confirmed by reverse phase HPLC, using a C4 column (300) and the solvent system based on 0.1 M TEAA buffer, pH 7.0 and acetonitrile (*13*). In addition, samples of the alkylated templates were 5′-labeled with ^{32}P and analyzed for purity on 18% PAGE−8 M urea high-resolution sequencing gel.

5′-Labeling of Oligonucleotides with ^{32}P. The primer oligonucleotides were labeled using 18 pmol of DNA and 20 μCi [γ-^{32}P]ATP (3000 Ci/mmol) together with 20 units of PNK (10 000 U/mL) in a reaction mixture containing the buffer for PNK provided by the company and BSA (100 μg/mL). The reaction of 5′-phosphorylation was performed at 37 °C for 1 h and 50 min, and the kinase was inactivated by incubation at 65 °C for 15 min.

5′-Labeling of Oligonucleotides with Nonradioactive P for Ligation. The oligonucleotides required to be 5′-phosphorylated for further ligation experiments were phosphorylated using 6 nmol of DNA and 20−30 units of T4 PNK in a buffer used in ligation experiments at 1 mM final ATP concentration under the same conditions as above.

Primer Extension Assay. All primer extension reactions were performed under steady state conditions. The substrates for the in vitro polymerase assay consisted of unmodified (control) and site specifically alkylated templates annealed with shorter complementary ^{32}P-labeled primers to form complexes **17**−**19** (Scheme 4). The reaction mixture contained 150−200 nM final duplex DNA concentration, primer:template (1:1.5 molar ratio) in buffer 1× for different DNA polymerases: 50 mM Tris-HCl, pH 7.5, 1 mM EDTA, 5 mM $MgCl_2$, 50 mM NaCl, and 1 mM DTT for T7 (exo-) DNA polymerase; 10 mM Tris-HCl, pH 7.5, 5 mM $MgCl_2$, and 7.5 mM DTT for Klenow (exo-) polymerase; and 40 mM Tris-HCl, pH 8.0, 10 mM $MgCl_2$, 60 mM KCl, and 10 mM DTT for polymerase η. Each buffer contained in addition 100 μg/mL BSA final concentration. The enzymes were added to the annealed primer/template complex such that their final concentration in the reaction mix was 15−20 nM (10-fold excess DNA substrate vs enzyme) except for polymerase η where the enzyme was 40 nM and the duplex DNA substrate was 200 nM such that the substrate:enzyme ratio was 5:1. The polymerase reaction was initiated by adding to the preformed (duplex DNA/polymerase) complex in an equimolar mixture of the four dNTPs in a range of 100−500 μM concentration of each (20−25 μL final volume of reaction). Equal aliquots from the reaction mix (5−7 μL at each time point) were withdrawn at 1, 3, 5, 10, and 30 or 60 min and quenched with an equal volume (5−7 μL) mixture of 20 mM EDTA, pH 8.0, and sequencing loading gel buffer containing 95% formamide and 0.05% bromphenol blue. Fractionation of all products from the primer extension reaction was performed by PAGE and quantified as described above.

Single Nucleotide (nt) Incorporation Assay. Four independent reactions, corresponding to the incorporation of dATP, dGTP, dCTP, and dTTP opposite the lesions, were run at 250−500 μM dNTP concentration using the same procedure and enzymes described for the primer extension assay using the DNA substrate constructs **20**−**22**.

Construction of M13 Genome Containing a Single 2,7-DAM-dG-N7 Adduct (8) and Replication in *E. coli*. Construction of the modified and control M13 genome involved digestion of M13mp7L2 single-stranded DNA with *Eco*RI, annealing a 50-mer scaffold, and ligation of the 2,7-DAM-dG-N7 containing and control 10-mer, which followed the protocol described earlier in detail (*14*, *16*) (Figure S1, Supporting Information). Briefly, 400 μg of bacteriophage M13mp7L2 DNA was digested with 3200 units of *Eco*RI for 2 h at 25 °C in 1 mL of 100 mM Tris-HCl, pH 7.5, 5 mM $MgCl_2$, and 50 mM NaCl. An equimolar ratio of a scaffold 50-mer, which contained deoxyuridines in place of thymidines, was annealed to the linear ss DNA at a concentration of 100 ng/mL by heating at 75 °C for 15 min followed by slow cooling to room temperature over a period of 3−4 h. A 10-fold molar excess of the modified (*13*) or unmodified 5′-phosphorylated 10-mer was ligated into the gap of this annealed DNA in the presence of 800 units of T4 DNA ligase in 40 mM Tris-HCl buffer (pH 7.8), 8 mM $MgCl_2$, 16 mM DTT, and 1 mM ATP at 16 °C for 48 h. After ethanol precipitation, an additional round of *Eco*RI (5 units/μg DNA) digestion was carried out for 4 h to linearize any uncut or religated DNA. The efficiency of ligation was ∼34% for both the control and the modified 10-mer. To remove the 50-mer scaffold from the M13 DNA, the uracil sites in the scaffold were converted to abasic sites by uracil DNA glycosylase (UDG), whereas exonuclease III treatment cleaved the abasic sites and digested the scaffold oligomer. The resulting constructs were run on 1% agarose gel, and the circular DNA bands were quantitated using the KODAK Digital Science 1D program.

Repair-competent *E. coli* (DL7) cells were grown in 100 mL cultures in Luria broth to 1 × 10^8 cells/mL and were made electrocompetent with and without SOS induction using UV light (254 nm) (20 J/m^2) as described (*14*, *16*). For each transformation, 60 μL of the cell suspension was mixed with 60 ng of M13 construct and transferred to the bottom of an ice-cold Bio-Rad Gene-Pulser cuvette (0.1 cm electrode gap). Electroporation of cells was carried out in a Bio-Rad Gene-Pulser apparatus at 25 μF and 1.8 kV with the pulse controller set at 200 Ω. Following a 1 h recovery at 37 °C, the cells were centrifuged to isolate the phage-containing supernatant. Analysis of progeny phage was carried out by oligonucleotide hybridization (*14*, *16*).

Construction of Single-Stranded pMS2 Shuttle Vector Containing a Single 2,7-DAM-dG-N7 Adduct 8 and Replication in Simian Kidney Cells. The single-stranded pMS2 shuttle vector, which contains a hairpin region similar to M13mp7L2, was prepared as described (*17*). The pMS2 DNA

(58 pmols, 100 g) was digested with a large excess of *Eco*RV (300 pmol, 4.84 g) for 1 h at 37 °C followed by room temperature overnight. A 56-mer scaffold oligonucleotide was annealed overnight at 9 °C to form the gapped DNA. 5′-Phosphorylation and ligation of the control and 2,7-DAM-dG-N7-containing 10-mers to pMS2 DNA (*13*) were carried out similarly as that for M13 DNA described above. Unligated oligonucleotides were removed by passing through Centricon-100, and the DNA was precipitated with ethanol. The scaffold oligonucleotide was digested by treatment with T4 DNA polymerase and exonuclease III, the proteins were extracted with phenol/chloroform, and the DNA was precipitated with ethanol. The final construct was dissolved in 1 mM Tris-HCl−0.1 mM EDTA, pH 8, and a portion was subjected to electrophoresis on 1% agarose gel in order to assess the amounts of circular DNA.

COS-7 cells were grown in Dulbecco's modified Eagle medium supplemented with 10% fetal calf serum. The cells were seeded at 5×10^5 cells per 60 mm plate. Following overnight incubation, the cells were transfected with 100 ng of ss DNA by electroporation. The culture was incubated for 2 days, and the progeny plasmid was recovered by the method of Hirt. It was then used to transfect *E. coli* DH10B, and transformants were analyzed by oligonucleotide hybridization (*14*).

Results

Construction of M13 and pMS2 Constructs. The construction of site specifically modified M13 and pMS2 vectors followed a protocol originally developed by Lawrence and co-workers (*19*) and used extensively by us and others (*14*, *16*, *17*) (Figure S1, Supporting Information).

Thermal Stability of 2,7-DAM-dG-N7 Adduct 8. Adducts at the N7 position of 2′-deoxyguanosine destabilize the glycosidic bond. Indeed, the half-life of the 2,7-DAM-dG-N7-adducted decamer was less than 3 min at 90 °C and the major product formed by the release of 2,7-DAM-Gua-N7 was an abasic site-containing oligonucleotide (Figure S2, Supporting Information). However, the 2,7-DAM-dG-N7 adduct was shown to be remarkably stable in duplex DNA under physiological conditions: its half-life at 25 and 37 °C is 400 and 96 h, respectively (*8*).

Because an abasic site is a well-known mutagenic lesion (*18*, *19*), we considered it particularly important to ensure that the M13 phage with the 2,7-DAM-dG-N7 construct did not contain a significant amount of this byproduct. Following construction of the M13 vectors, the scaffold, which contained several deoxyuridines, was then removed by UDG followed by exonuclease III treatment. For the pMS2 vectors, the scaffold was digested with T4 DNA polymerase and exonuclease III. The enzymatic scaffold removal should also convert circular genomes with abasic sites to linear molecules, which was tested by ligating an abasic site containing decamer into M13 DNA followed by exonuclease III treatment. Indeed, subsequent analysis by agarose gel electrophoresis showed that the circular genome was completely converted to linear DNA (data not shown). For the 2,7-DAM-dG-N7-containing genome, however, similar analysis exhibited less than 5% difference in the amount of circular construct, which suggests that 2,7-DAM-dG-N7 is stable during the experimental manipulations in the more hydrophobic milieu of the single-stranded M13 genome (or any other large DNA) (Figure 2). For example, lanes 3 and 4 in Figure 2 represent typical constructs containing 2,7-DAM-dG-N7 (**8**) and control-dG, respectively, after removal of the scaffold, whereas lane 5 shows the same for a "mock" construct in which no oligonucleotide was added during the ligation step.

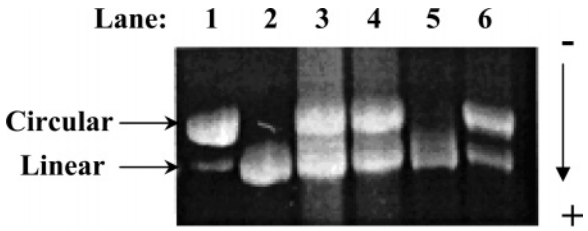

Figure 2. Analysis of M13 DNA constructs by 1% agarose gel electrophoresis. Lanes 1 and 2 show DNA before and after digestion with *Eco*RV. Lanes 3 and 4 show constructs containing 2,7-DAM-dG-N7 and control-dG, respectively, after enzymatic removal of the scaffold. Lane 5 and 6 show after and before the removal of the scaffold, respectively, of a mock ligation mixture, which did not contain a decamer.

Table 1. Toxicity of 2,7-DAM-dG-N7-Modified M13 Phage in *E. coli*

	relative survival (%)		
host	M13-dG (control)	M13-DAM-dG (modified)	M13-MC-dG monoadduct[a]
E. coli − SOS	100	54 ± 13	∼7
E. coli + SOS	100	51 ± 14	∼12
E. coli (uvr⁻) − SOS	100		∼0.2−2
E. coli (uvr⁻) + SOS	100		∼2−8

[a] Data from ref *14*.

Biological Effects of 2,7-DAM-dG-N7. Replication of the modified and control M13 genome in *E. coli* showed that the presence of 2,7-DAM-dG-N7 lowered the viability by approximately 50%, suggesting that the lesion stalls translesion synthesis (TLS) but does not block it to a significant extent. The viability was 54 ± 13% without and 51 ± 14% with SOS (10 J/m^2), which suggests that TLS past 2,7-DAM-dG-N7 does not increase in SOS-induced cells. When compared with the single guanine N^2 monoadduct of MC **7** in M13, which exhibited viability of ∼7 and 12% for uninduced and SOS-induced (10 J/m^2) cells, respectively, 2,7-DAM-dG-N7 appears to be a much less toxic lesion (Table 1). Other studies in mouse mammary tumor cells indicated that 2,7-DAM is much less cytotoxic than MC and DMC (*9*, *10*, *20*). For screening potential mutant progeny, we used oligonucleotide hybridization using a 17-mer probe complementary to the region where the 10-mer was inserted. The probe was designed to bind to nonmutant plaques, and any plaques that did not hybridize or hybridized weakly were subjected to DNA sequencing.[3] Of the 4342 plaques (1203 without SOS and 3139 with SOS) screened, no mutants were identified from 2,7-DAM-dG-N7 construct as was the case with the control construct (Table 2). The mutation frequency of 2,7-DAM-dG-N7, therefore, was less than 2×10^{-4}.

To investigate if this adduct is mutagenic in mammalian cells, we constructed a pMS2 shuttle phagemid vector containing the adduct. Biological effects of many DNA damages have been studied by using this vector (*17*, *21*, and references therein), and the strategy for employing this plasmid is similar to the M13 construct described

[3] Initially, in addition to the wild-type probe, we used probes to detect each of the three targeted base substitutions. Because of our failure to detect any targeted base substitutions, however, later, we concentrated entirely on the nonmutant probe, which would detect, in addition to base substitutions, small frameshifts and semitargeted mutations.

Table 2. Analysis of Progeny from 2,7-DAM-dG-N7 and Control Vector Replication in *E. coli* (DL7) and COS-7 Cells

construct	host	no. progeny screened	total G	no. of mutants	type of mutations	% mutations
M13-dG	*E. coli* (− SOS)	1457	1457	0		<0.07
M13-2,7-DAM-dG-N7	*E. coli* (− SOS)	1203	1203	0		<0.08
M13-dG	*E. coli* (+ 10 J/m^2)	1270	1270	0		<0.08
M13-2,7-DAM-dG-N7	*E. coli* (+ 10 J/m^2)	3139	3139	0		<0.03
pMS2-dG	COS-7	305	303	2	"A" del, 5 b 3′ to G	0.66
pMS2-2,7-DAM-dG-N7	COS-7	395	394	1	"G" insertion next to G*	0.25

above. Briefly, the pMS2 single-stranded DNA was digested with *Eco*RV and the linear DNA was hybridized with a 56-mer scaffold to yield a gapped DNA. The decamers containing either 2,7-DAM-dG-N7 or dG were ligated to this gap. The control and 2,7-DAM-dG-N7 constructs were treated with exonuclease III and T4 DNA polymerase to remove the scaffold. Following purification, the site specifically altered pMS2 vectors were transfected in COS-7 cells by electroporation. The transformants were analyzed by oligonucleotide hybridization followed by DNA sequencing. For the 2,7-DAM-dG-N7 construct, of the 395 progeny screened, we detected one mutant, which contained a +1 frameshift adjacent to the adducted G (MF < 0.25%) (Table 2). For the control, we have isolated two mutants within the inserted decamer sequence after screening 305 colonies (MF < 0.66%) (Table 2). Therefore, mutational frequency of 2,7-DAM-dG-N7 in COS-7 cells was not higher than the spontaneous mutation frequency.

Primer Extensions on Adducted Templates. Design and Construction of Templates (Scheme 3). The short adducted oligonucleotides **10**−**13** were designed for ligase-mediated extension to 24- or 27-mer template strands **14**−**16**. They were isolated by HPLC from alkylation reaction mixtures as described in the Methods section. Each was further purified and shown to be homogeneous on HPLC (Figure S3, Supporting Information). The digest of each adducted oligo showed the presence of the expected adduct: **7** or **8** (Figure S4, Supporting Information). The expected adduct and nt compositions of **10**−**13** were verified by ESI-MS (Table S1, Supporting Information). The positions of the 2,7-DAM-adduct **8** in **11**−**13** had to be independently determined, since these oligonucleotides contained more than one alkylatable target guanines, necessitated by the known sequence selectivity of formation of adduct **8** upon alkylation of DNA by 2,7-DAM. The alkylation is selective in general for G tracts of DNA and for the 3′-G in −NGGN− sequences in duplex oligonucleotides; guanine in −NGN− sequences is essentially unreactive (*15*, *22*). Accordingly, each of the oligonucleotide substrates for 2,7-DAM alkylation was designed to contain the same −TGGTA− target sequence. The oligonucleotide substrate for **13** contained an additional guanine in an −AGT− sequence, which was not expected to be alkylated. The positions of the adduct in **11**−**13** were determined experimentally by PAGE assay of their fragmentation upon treatment with hot piperidine (*23*). The assay applied previously to **11** has shown position 4 as the site of the adduct **8** (*15*). Similarly, assay of the new adducted oligonucleotide **12** showed now that adduct **8** was located exclusively at nt position 4, as expected (Figure 3a). The same assay of **13**, which has three Gs, indicated that the 2,7-DAM adduct **8** was located in nt position 7 (Figure 3b).

The templates **14**−**16** were designed to contain the adduct located close to the 5′ terminus in order to ensure uninhibited initial binding of the primer−template duplex substrate (Scheme 4) to the DNA polymerases. These templates were homogeneous on HPLC and PAGE (Figures S5 and S6, respectively, Supporting Information) and showed the expected composition by ESI-MS (Table S1, Supporting Information).

Primer Extension on MC-Adducted Template 14 (Adduct 7) and 2,7-DAM-Adducted Template 16 (Adduct 8) by Klenow (exo-) DNA Polymerase. The primer strand in MC complex **17** containing adduct **7** (Scheme 4) was elongated only up to 19-mer, indicating a complete stop of elongation one nt before the MC adduct **7** in the template (Figure 4a). Rates and extent of the elongation relative to the unmodified control complex are shown in Figure 4b, and these results indicate that the

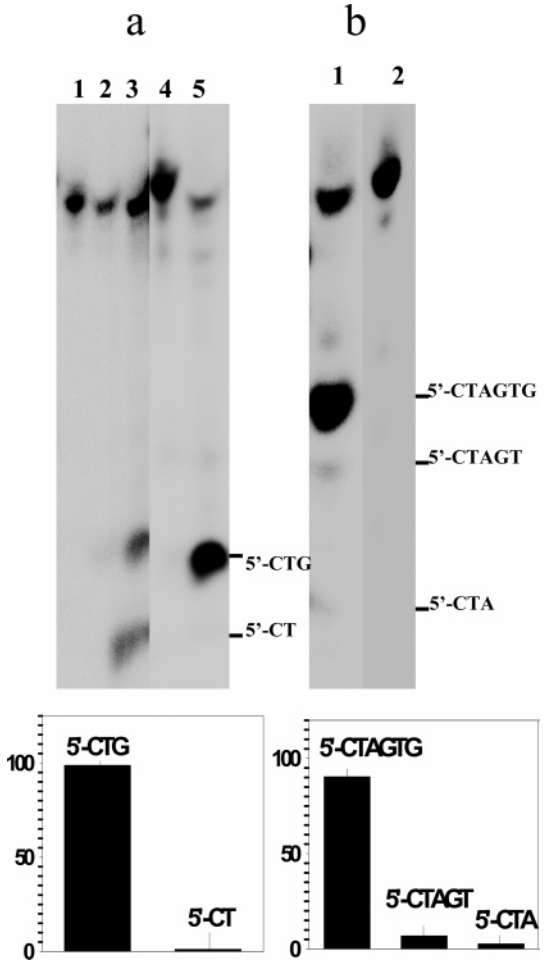

Figure 3. Piperidine cleavage assay of the 2,7-DAM-N7 adduct (**8**) positions in the alkylated oligonucleotides **12** and **13**. (a) Assay of **12**: PAGE (top) and histogram of % relative fragment intensities in lane 5 (below). PAGE lanes: 1, control; 2, control + piperidine; 3, control + dimethyl sulfate (DMS) + piperidine (G-lane); 4, **12**; 5, **12** + piperidine. (b) Assay of **13**: PAGE (top) and fragment intensities (below). PAGE lanes: 1, **13** + piperidine; 2, **13**.

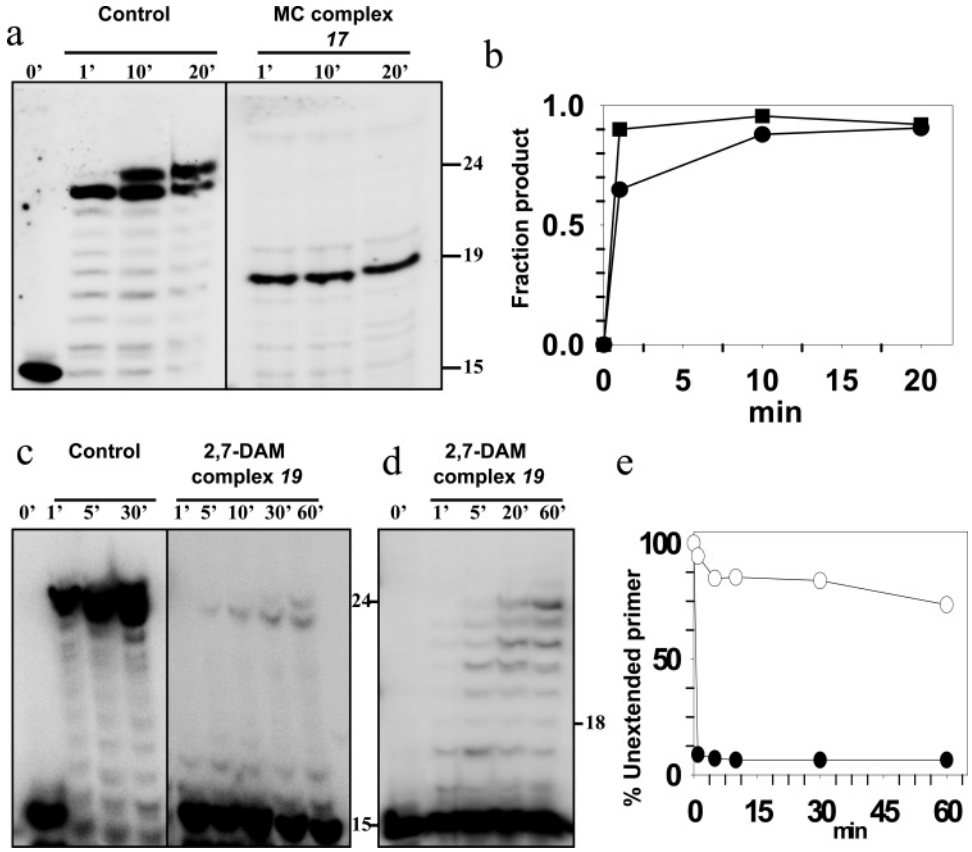

Figure 4. PAGE analysis of primer extension of MC-dG-N^2- and 2,7-DAM-dG-N7-adducted templates by Klenow (exo-) DNA polymerase. The MC complex **17** contains adduct **7**, and the 2,7-DAM complex **19** contains adduct **8**. (a) PAGE of primer extension in MC-adducted template/primer complex **17**. Reaction conditions: 250 μM dNTP (each), 200 nM complex **17**, 40 nM Klenow (exo-) DNA polymerase; 25 °C. Minutes of incubation time are indicated above each lane. (b) Plots of results in panel a. The fraction of the expected 24-mer fully extended product (control) and aborted 19-mer product (1 nt before MC lesion) is plotted as a function of incubation time (●, 24-mer control product; ■, 19-mer abortive product). (c) PAGE of primer extension of 2,7-DAM-dG-N7-adducted template/primer complex **19**. Reaction conditions: 250 μM dNTP (each), 200 nM complex **19**, 40 nM Klenow (exo-) DNA polymerase (S:E ratio, 5:1); 25 °C. Minutes of incubation time are indicated above each lane. (d) Same as panel c, except only 40 nM complex was used (S:E ratio, 1:1). (e) Plots of results in panel d. The percent of original primer that remained unextended during the primer extension reaction is plotted as a function of incubation time. The 2,7-DAM lesion (○) is bypassed with a slower rate as compared with the control undamaged template (●).

rate of progress of the extension up to their termination length is approximately the same for both complexes.

The primer strand in the 2,7-DAM complex **19** containing adduct **8** was elongated past the 2,7-DAM adduct **8**. This is concluded from the presence of 18−24 nt long primer products at gradually increasing relative intensities of the fully extended 24-mer as the time of the incubation was increased from 1 to 60 min (Figure 4c). This extension reaction was conducted at a 5:1 stoichiometry of the duplex **19**:enzyme ratio. Another extension reaction was run at 1:1 stoichiometry, which resulted in a slightly different pattern, in which some accumulation of intermediates between 17- and 23-mers was detected (Figure 4d). In any case, both results indicate that the 2,7-DAM-dG-N7 adduct **8** is bypassed by Klenow (exo-) DNA polymerase, in contrast to the MC-dG-N^2 adduct **7**. It is notable, however, that the rate of disappearance of the starting 15-mer primer is much slower than that in the nonadducted control complex or in the MC-adducted complex **17**.

Primer Extension on MC-Adducted Template 14 (Adduct 7) and 2,7-DAM-Adducted Template 16 (Adduct 8) by T7 (exo-) DNA Polymerase. The primer strand in the MC complex **17** was again elongated only to a 19-mer, indicating a complete block of elongation one nt before the MC adduct **7** in the template (Figure 5a). This polymerase exhibited a low activity for elongation of the starting 15-mer primer in complex **17** relative to elongation of the control, nonadducted complex and also relative to elongation in complex **17** by Klenow (exo-) DNA polymerase. In sharp contrast, the primer strand in the 2,7-DAM-dG-N7 complex **19** was elongated to full its 24 nt length, indicating bypass of the adduct **8** in the template, albeit at a lower efficiency relative to the control, nonadducted template (Figure 5b). A similar result was obtained using complex **18** as the substrate for the T-7 (exo-) polymerase as shown in Figure S7b, Supporting Information. This substrate yielded, in addition, products of overextension of the primer by 1, 2, or 3 nts beyond the template terminus, most likely originating from primer slippage.

Primer Extension on MC-dG-N^2-Adducted Template 14 and 2,7-DAM-dG-N7-Adducted Template 16 by Polymerase η. In the MC-dG-N^2 complex **17**, polymerase η extended the primer strand only to 19-mer, one nt before the MC adduct **7** in the template strand, at relatively low efficiency as compared to control primer extension (Figure 6a). In contrast, in the 2,7-DAM-dG-N7 complex **19**, the primer strand was extended two nts past the 2,7-DAM adduct **8**, to 20-mer, with surprisingly high efficiency. A product corresponding to the fully extended primer is formed only to a low extent (Figure

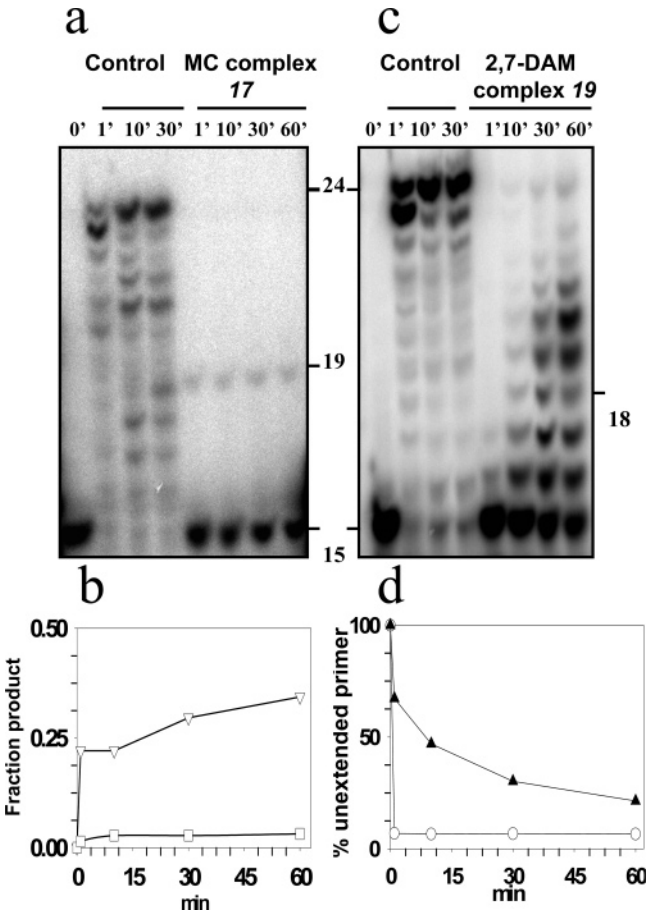

Figure 5. PAGE analysis of primer extension on MC-dG-N^2- and 2,7-DAM-dG-N7-adducted templates by T7 (exo-) DNA polymerase. The MC complex **17** contains adduct **7**, and the 2,7-DAM complex **19** contains adduct **8**. (a) PAGE of primer extension of MC-adducted template/primer complex **17**. Reaction conditions: 250 μM dNTP (each), 200 nM complex **17**, 40 nM T7 (exo-) DNA polymerase; 25 °C. Minutes of incubation time are indicated above each lane. (b) Plots of results in panel a. The fractions of the expected 24-mer fully extended control product (▽) and an aborted 19-mer product (1 nt before MC adduct) (□) are plotted as a function of incubation time. The rates for the two products are different. The MC adduct is not bypassed, and a 19-mer aborted product (1 nt before lesion) is accumulated at a slower rate than in the case of the same reaction run with Klenow (exo-) DNA polymerase (see Figure 4b). (c) PAGE of primer extension of 2,7-DAM-dG-N7-adducted template/primer complex **19**. Reaction conditions: Same as in panel a. (d) Plots of results in panel c. The percent of original primer that remained unextended during the primer extension reaction is plotted as a function of incubation time for the complex **19**. The 2,7-DAM adduct (▲) is bypassed with a slower rate than the control undamaged template (○).

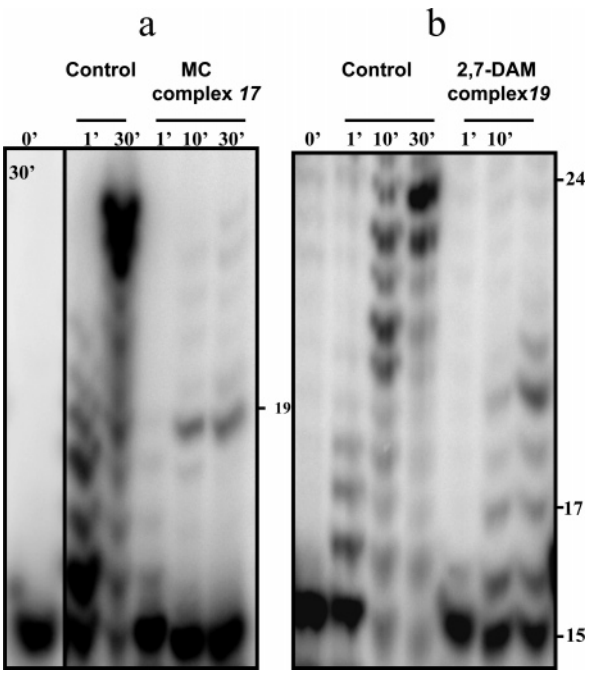

Figure 6. PAGE analysis of primer extension on MC-dG-N^2- and 2,7-DAM-dG-N7-adducted templates by DNA polymerase η. The MC complex **17** contains adduct **7**, and the 2,7-DAM complex **19** contains adduct **8**. (a) PAGE of primer extension of MC-adducted template/primer complex **17**. Reaction conditions: 250 μM dNTP (each), 200 nM complex **17**, 40 nM DNA polymerase η; 25 °C. (b) PAGE of primer extension of 2,7-DAM-adducted template/primer complex **19**. Reaction conditions: as in panel a. The mark 17 represents the position of the primer extended to 1 nt before the adduct.

6b). In these reactions, a ratio of 5:1 (S:E) was employed. In analogous studies of other bulky adducts, polymerase η showed similarly low efficiencies of primer extension under such conditions (*32*, *33*). However, using a lower (3:1) S:E ratio, we observed substantially more efficient TLS and the extension to 23 nt length of the primer (Figure S8 Supporting Information).

Single Nt Incorporation Opposite a 2,7-DAM-dG-N7 Adduct (8). These experiments were designed to test the fidelity of the translesion bypass observed in the case of the 2,7-DAM-adducted (**8**) templates, described above. The alkylated primer−template complex **21** and the control nonalkylated complex were incubated with only a single dNTP at a time at high concentration (500 μM) and Klenow (exo-) DNA polymerase. The control non-alkylated complex incorporated two C units into the primer strand (25-mer). A small amount of primer intermediate (24-mer) incorporating one single C unit was observed at the end of the 60 min incubation period (Figure 7b). No appreciable incorporation of the other three nts was observed (data not shown). The alkylated complex **21** incorporated two C units at a lower overall efficiency than the control (Figure 7a). The 24-mer one C-incorporated intermediate was accumulated in a 2-fold proportion relative to the 25-mer two C product, during the 60 min incubation (Figure 7c). Figure 7a shows that the nts A and T were not incorporated. The base G was incorporated to a relatively low extent opposite the G(4) position of the template. The important conclusion of these results is that the 2,7-DAM-guanine-N7 adduct **8** is not mutagenic in the Klenow (exo-) DNA polymerase replication system.

Discussion

In light of the lack of cytotoxicity of the MC metabolite and bulky DNA alkylator 2,7-DAM, the present experiments were designed to assess the biological properties of its major 2,7-DAM-DNA adduct. In particular, we tested the hypothesis that the guanine-N7 monoadduct of 2,7-DAM (**8**) is relatively noninhibitory to DNA replication and its fidelity, which could account for the low toxicity of the parent drug, 2,7-DAM. The structurally similar guanine-N^2 monoadduct of MC (**7**) was used as a benchmark since this adduct was found to be cytotoxic and strongly inhibitory to DNA replication in our earlier study (*13*, *14*). Comparison of the two adducts also promised to lead to a better understanding of DNA

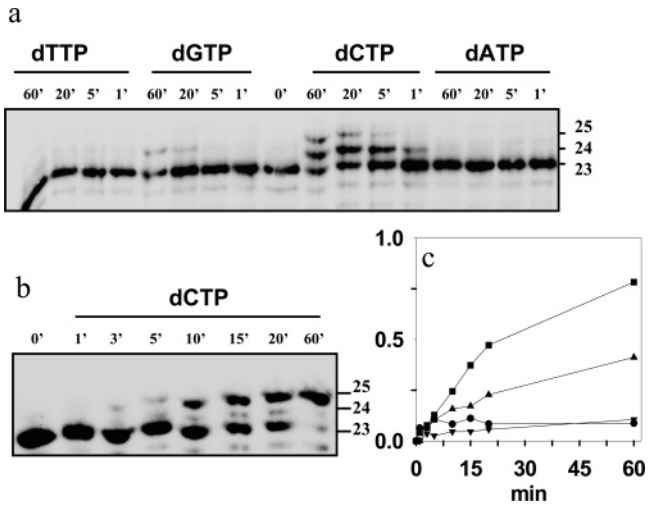

Figure 7. PAGE analysis of single nt incorporation into the primer opposite the 2,7-DAM dG-N7 adduct **8** in the drug-modified template strand of complex **21** by Klenow (exo-) DNA polymerase. (a) PAGE of incorporation of each of four dNTPs into complex **21**. Reaction conditions: 500 μM dNTP, 200 nM complex **21**, and 20 nM Klenow (exo-) DNA polymerase; 25 °C. Minutes of incubation time are indicated above the lanes. Conditions: same as in panel a. (b) PAGE of incorporation of dCTP in the nonalkylated control for complex **21**. Conditions: same as in panel a. Minutes of incubation time are indicated above the lanes. (c) Plots of results from panels a and b. The fraction of product for the 24- and 25-mer extended primer products is plotted as a function of incubation time for both the control and the 2,7,DAM-damaged template reactions. The 24-mer one-C-incorporated intermediate was accumulated in a 2-fold proportion relative to the 25-mer two-C-product, during the 60 min incubation. ■, nonalkylated control 25-mer; ▲, adducted template/primer 24-mer; ●, adducted template/primer 25-mer; and ▼, nonalkylated control 24-mer.

adduct−structure activity relationships in the mitomycin drug family.

Indeed, the results show clearly that the 2,7-DAM-dG-N7 adduct **8** inhibits the replication of the M13 phage genome in *E. coli* only weakly, in contrast to the MC-dG-N^2 DNA adduct **7**, which is a strong inhibitor (Table 1). Furthermore, the replication fidelity of adduct **8** is unimpaired, as seen from the lack of any mutant progeny generated in *E. coli* (SOS$^-$ or SOS$^+$) and COS-7 cells (Table 2). These experiments in vivo were complemented by primer extension assays in vitro. The DNA polymerases Klenow (exo-) and T7 (exo-) were able to extend the primer strands past the position of the 2,7-DAM-dG-N7 adduct **8** in synthetic templates, although at slower rates than in the control experiments, while the MC-dG-N^2 adduct **7** posed an absolute block to primer extension by both, in agreement with our previous findings (*13*). Furthermore, the 2,7-DAM-dG-N7 adduct directed the incorporation of only the nonmutagenic base C when catalyzed by Klenow (exo-) DNA polymerase. These results are in excellent agreement with those obtained in the *E. coli* and COS-7 in vivo systems. Taken together, the results are consistent with the hypothesis that the 2,7-DAM-dG-N7 adduct poses only a weak block to the replication of DNA and is intrinsically nonmutagenic; furthermore, they suggest that these innocuous properties of the major DNA adduct **8** account for the lack of biological activity of the parent drug 2,7-DAM itself. However, it is possible that in intact cells additional mechanisms also contribute to the observed results; in particular, differential rates of repair of the G-N7 (**8**) and G-N^2 (**7**) lesions. The site specific G-N7 adduct in the M13 phage construct may be repaired more rapidly than the G-N^2 adduct. We found previously that the toxicity of the latter was slightly modulated by various *uvr* repair mutations in the *E. coli* host although in view of the single-stranded structure of the M13 construct, these effects could not be fully interpreted (*14*). No comparative experiments involving the M13 construct with adduct **8** have been conducted so far.

What structural factors may be responsible for the observed contrast between the 2,7-DAM-dG-N7 adduct **8** and the MC-dG-N^2 adduct **7** as replication blocks? The three-dimensional solution structure of the G-N7 adduct **8** in duplex DNA (*15*) indicated that the drug moiety is not intercalated and lies in the major groove of a relatively nonaltered B-DNA structure. In contrast, the mitomycin drug moiety of the G-N^2 adduct **7** lies snugly in the minor groove of duplex DNA (*27*). Although solution structures of primer−template junctions at mitomycin adducts have not been determined experimentally, we may speculate, based on the adducted duplex DNA structures above that at this junction the Watson−Crick H-bonding interface of the G-N7 adduct in the template and the incoming dNTP is unobstructed; furthermore, the drug moiety of the adduct has no tendency to stack with the incoming dNTP and the guanine when this basepair is formed. Rather, the drug moiety stays out of the way in the incipient major groove during the TLS step at the active site. In contrast, the H-bonding interface of the G-N^2 adduct in the template is directly obstructed by the bound drug moiety and formation of the closed conformation of the DNA polymerase (*28*) is sterically prevented.

A similar scenario was proposed for an earlier precedent, which is analogous to the present findings (*29*): The ethylene dibromide-derived bulky glutathione adducts at the N7- and N^2-positions of guanine differ considerably in their behavior in TLS systems of all four DNA polymerases tested. The N7 adduct allowed relatively efficient full primer extension and selective incorporation of dCTP opposite the adduct, while the N^2 adduct strongly blocked replication and only dATP was incorporated opposite to the adduct. The authors suggested a similar explanation to what we propose above and speculated that the weak blocking effect of the G-N7 adduct is due to direct interaction of the bulky glutathione residue with the polymerases.

A structurally different class of bulky guanine-N7 adducts is known in which the drug moiety is intercalated between two base pairs. Examples of this class are aflatoxin B$_1$ (*24*) and the pluramycins (*30*). Relevant studies on TLS in vitro of these lesions are scarce, due to the general instability of the adducts. In an in vivo study analogous to that presented here, the cytotoxicity and mutational properties of the primary AFB$_1$-guanine-N7 DNA adduct were investigated in *E. coli* transfected with an M13 phage construct containing a site specifically placed single adduct in the genome of the phage. In contrast to the 2,7-DAM-guanine-N7 adduct, this adduct was highly cytotoxic and mutagenic (*31*). Members of the pluramycin drug family, known to form intercalated DNA adducts, are intensely cytotoxic (*30*). On the basis of these considerations and our present results, it appears that bulky G-N7 adducts, which intercalate in duplex DNA, inhibit DNA replication and its fidelity while groove-binding G-N7 adducts are less inhibitory.

Although the structural details and biological function of the translesion bypass type DNA polymerase η differ from those of the T7 and Klenow fragment polymerases (*25*), the observed differential extent of the bypass of the 2,7-DAM-dG-N7 and MC-dG-N^2 adducts in the cell free system (Figure 6) follows the same adduct structure−activity pattern obtained using the other two DNA polymerases.

The cytotoxin MC is the product of evolution in *Streptomyces*, the producing microorganism. Several self-protective MC detoxification pathways operating within *Streptomyces* have been discovered (*26*). Considering that reduction of MC in vivo or in vitro converts most of the drug to the nontoxic quinone 2,7-DAM (Scheme 2a; *2*, *3*), this process may be regarded as an additional detoxification mechanism. We showed now that the detoxification of MC by this pathway is not simply due to conversion of the drug from DNA cross-linker to DNA monoalkylator but, beyond this, the intrinsic nontoxicity of the resulting DNA monoadduct.

Although the reduction of MC generates the MC hydroquinone **3**, the common precursor leading to the toxic and nontoxic pathways, the partitioning of **3** favors greatly the latter. Enhancement of the toxic pathway of MC to the detriment of its conversion to the nontoxic 2,7-DAM should lead to a higher efficacy of MC as a cancer drug against tumor cells. However, it is difficult to envision how this may be achieved by some manipulation of the cellular environment (*6*).

Acknowledgment. We are grateful to Dr. Masaki Moriya (SUNY, Stony Brook) for providing pMS2 shuttle vector and to Drs. Thomas A. Kunkel and Scott McCulloch (NIEHS) for their generous gift of DNA polymerase η. Dr. Cliff Soll (Hunter College) is acknowledged for expert mass spectroscopy analysis of template oligonucleotides. This study was supported by NIEHS Grants ES09127 (to A.K.B.), NCI Grant CA41086 (to M.T.), Grant 440828 from the University of Connecticut Research Foundation (to A.K.B.), and a Research Centers in Minority Institutions Award RR-03037 from the National Center for Research Resources, NIH, which supports the infrastructure of the Chemistry Department of Hunter College; the contents are solely the responsibility of the authors and do not necessarily represent the official views of the NCRR/NIH.

Supporting Information Available: General scheme of construction, replication, and analysis of the control and modified vector; depurination kinetics of a 2,7-DAM adduct **8**-containing decamer at 90 °C; results of purity analyses of **10**−**16**; additional PAGE analyses of primer extension on 2,7-DAM **8**-adducted templates; and data of ESI-MS (−) analyses of various oligonucleotides used in the work. This material is available free of charge via the Internet at http://pubs.acs.org.

References

(1) Carter, S. K., and Crooke, S. T. (1979) *Mitomycin C, Current Status and New Developments*, Academic Press, New York.

(2) Chirrey, L., Cummings, J., Halbert, G. W., and Smyth, J. F. (1995) Conversion of mitomycin C to 2,7-diaminomitosene and 10-decarbamoyl 2,7-diaminomitosene in tumor tissue in vivo. *Cancer Chemother. Pharmacol. 35*, 318−322.

(3) Tomasz, M., and Lipman, R. (1984) Reductive metabolism and alkylation activity of mitomycin C induced by rat liver microsomes. *Biochemistry 20*, 5056−5061.

(4) Tomasz, M. (1995) Mitomycin C: Small, fast and deadly (but very selective). *Chem. Biol. 2*, 575−579.

(5) Szybalski, W., and Iyer, V. N. (1967) In *Antibiotics I: Mechanism of Action* (Gottlieb, D., and Shaw, P. D., Eds) p 230, Springer-Verlag, New York.

(6) Suresh Kumar, G., Lipman, R., Cummings, J., and Tomasz, M. (1997) Mitomycin C DNA adducts generated by DT-diaphorase. Revised mechanism of the enzymatic reductive activation of mitomycin C. *Biochemistry 36*, 14128−14136.

(7) Palom, Y., Belcourt, M. F., Musser, S. M., Sartorelli, A. C., Rockwell, S., and Tomasz, M. (2000) Structure of adduct X, the last unknown of the six major DNA adducts of mitomycin C formed in EMT6 mouse mammary tumor cells. *Chem. Res. Toxicol. 13*, 479−488.

(8) Suresh Kumar, G., Musser, S. M., Cummings, J., and Tomasz, M. (1996) 2,7-Diaminomitosene, a monofunctional mitomycin derivative alkylates DNA in the major groove. Structure and basesequence specificity of the DNA adduct and mechanism of the alkylation. *J. Am. Chem. Soc. 118*, 9209−9217.

(9) Palom, Y., Belcourt, M. F., Suresh Kumar, G., Arai, H., Kasai, M., Sartorelli, A. C., Rockwell, S., and Tomasz, M. (1998) Formation of a major DNA adduct of the mitomycin metabolite 2,7-diaminomitosene in EMT6 mouse mammary tumor cells treated with mitomycin C. *Oncol. Res. 10*, 509−521.

(10) Palom, Y., Belcourt, M. F., Tang, L.-Q, Mehta, S. S., Sartorelli, A. C., Pritsos, C. A., Pritsos, K. L., Rockwell, S., and Tomasz, M. (2001) Bioreductive metabolism of mitomycin C in EMT6 mouse mammary tumor cells: Cytotoxic and noncytotoxic pathways, leading to different types of DNA adducts. The effect of dicumarol. *Biochem. Pharmacol. 61*, 1517−1529.

(11) Busby, W. F., Jr., and Wogan, G. N. (1984) Aflatoxins. In *Chemical Carcinogens* (Searle, C., Ed.) 2nd ed., pp 945−1136, American Chemical Society, Washington, DC.

(12) Hurley, L. H., and Needham-vanDevanter, D. R. (1986) Covalent binding of antitumor antibiotics in the minor groove of DNA. Mechanism of action of CC-1065 and the pyrrolo(1,4)benzodiazepines. *Acc. Chem. Res. 19*, 230−237.

(13) Basu, A. K., Hanrahan, C. J., Malia, S. A., Kumar, S., Bizanek, R., and Tomasz, M. (1993) Effect of site-specifically located mitomycin C-DNA monoadducts on in vitro DNA synthesis by DNA polymerases. *Biochemistry 32*, 4708−4718.

(14) Ramos, L. A., Lipman, R., Tomasz, M., and Basu, A. K. (1998) The major mitomycin C-DNA monoadduct is cytotoxic but not mutagenic in *Escherichia coli*. *Chem. Res. Toxicol. 11*, 64−69.

(15) Subramaniam, G., Paz, M. M., Suresh Kumar, G., Das, A., Palom, Y., Clement, C. C., Patel, D. J., and Tomasz, M. (2001) Solution structure of a guanine-N7-linked complex of the mitomycin C metabolite 2,7-diaminomitosene and DNA. Basis of sequence selectivity. *Biochemistry 40*, 10473−10484.

(16) Bacolod, M. D., Krishnasamy, R., and Basu, A. K. (2000) Mutagenesis of N-(deoxyguanosin-8-yl)-1-aminopyrene in a nonrepetitive CGC sequence in *Escherichia coli*. *Chem. Res. Toxicol. 13*, 523−528.

(17) Pandya, G., and Moriya, M. (1996) 1,N^6-Ethenodeoxyadenosine, a DNA adduct highly mutagenic in mammalian cells. *Biochemistry 35*, 11487−11492.

(18) Kunkel, T. A. (1984) Mutational specificity of depurination. *Proc. Natl. Acad. Sci. U.S.A. 81*, 1494−1498.

(19) Lawrence, C. W., Borden, A., Banerjee, S. K., and LeClerc, J. E. (1990) Mutation frequency and spectrum resulting from a single abasic site in a single-stranded vector. *Nucleic Acids Res. 18*, 2153−2157.

(20) Palom, Y., Suresh, Kumar, G., Tang, L.-Q., Paz, M. M., Musser, S. M., Rockwell, S., and Tomasz, M. (2002) Relative toxicities of DNA cross-links and monoadducts: New insights from studies of decarbamoyl mitomycin C and mitomycin C. *Chem. Res. Toxicol. 15*, 1398−1406.

(21) Moriya, M. (1993) Single-stranded shuttle phagemid for mutagenesis studies in mammalian cells: 8-oxoguanine in DNA induces targeted G.C → T.A transversions in simian kidney cells. *Proc. Natl. Acad. Sci. U.S.A. 90*, 1122−1126.

(22) Prakash, A. S., Beall, H., Ross, D., and Gibson, N. W. (1993) Sequence-selective alkylation and cross-linking induced by mitomycin C upon activation by DT-diaphorase. *Biochemistry 32*, 5518−5525.

(23) Hartley, J. A., and Wyatt, M. D. (1997) Determination of the DNA sequence specificity of alkylation damage using cleavage-based assays. In *Drug−DNA Interaction Protocols, Methods in Molecular Biology* (Fox, K. R., Ed.) Vol. 90, pp 147−156, Humana Press, Totowa, NJ.

(24) Gopalakrishnan, S., Harris, T. M., and Stone, M. P. (1990) Intercalation of aflatoxin B_1 in two oligonucleotide adducts:

Comparative ^{1}H. NMR analysis of d(ATC^{AFB}GAT).d(ATCGAT) and a(AT^{AFB}GCAT)$_2$. *Biochemistry 29*, 10438−10448.
(25) Kunkel, T. A., Pavlov, Y. I., and Bebenek, K. (2003) Functions of human DNA polymerases, and suggested by their properties, including fidelity with undamaged DNA templates. *DNA Repair 2*, 135−149.
(26) John, D. A., August, P. R., August, P. R., Shackleton, C., Liu, H., and Sherman, D. H. (1997) Microbial resistance to mitomycins involves a redox relay mechanism. *J. Am. Chem. Soc. 119*, 2576−2577.
(27) Sastry, M., Fiala, R., Lipman, R., Tomasz, M., and Patel, D. J. (1995) Solution structure of the monoalkylated mitomycin C-DNA complex. *J. Mol. Biol. 247*, 338−359.
(28) Steitz, T. A., Smerdon, S. J., Jager, J., and Joyce, C. M. (1994) A unified mechanism for nonhomologous DNA and RNA polymerases. *Science 266*, 2022−2025.
(29) Kim, M.-S., and Guengerich, F. P. (1998) Polymerase blockage and misincorporation of dNTPs opposite the ethylene dibromide-derived DNA adducts *S*-[2-(*N*7-guanyl)ethyl]glutathione, *S*-[2-(*N*^{2}-guanyl)ethyl]glutathione, and *S*-[2-(*O*^{6}-guanyl)ethyl]glutathione. *Chem. Res. Toxicol. 11*, 311−316.
(30) Hansen, M. R., and Hurley, L. H. (1996) Pluramycins. Old drugs having modern friends in structural biology. *Acc. Chem. Res. 29*, 249−258.
(31) Bailey, E. A., Iyer, R. S., Stone, M. P., Harris, T. M., and Essigmann, J. M. (1996) Mutational properties of the aflatoxin B_1-DNA adduct. *Proc. Natl. Acad. Sci. U.S.A. 93*, 1535−1539.
(32) Zhang, Y., Wu, X., Guo, D., Rechkoblit, O., Geacintov, N. E., and Wang, Z. (2002) Two-step error-prone bypass of the (+)- and (−)-*trans-anti*-BPDE-*N*^{2}-dG adducts by human DNA polymerases eta and kappa. *Mutat. Res. 510*, 23−25.
(33) Ling, H., Sayer, J. M., Plosky, B. S., Yagi, H., Boudsocq, F., Woodgate, R., Jerina, D. M., and Yang, W. (2004) Crystal structure of a benzo[*a*]pyrene diolepoxide adduct in a ternary complex with a DNA polymerase. *Proc. Natl. Acad. Sci. U.S.A. 101*, 2265−2269.

TX049813H